ENGINEERING RESEARCH JOURNAL (ERJ)

Vol. 1, No. 39 January 2019, pp. 79-85.

Journal Homepage: www.feng.bu.edu.eg

Heat Transfer Enhancement and Flow Structure in Heat Exchanger Tube By Using In-Line And Staggered Discrete Ribs Arrangements

Emad Z. Ibrahim, Mohamed A. Essa, Mostafa M. Ibrahim and Mohamed N. El-Sayed

Mechanical Power Engineering Department, Faculty of Engineering, Zagazig University, Zagazig, Egypt

Abstract

In the present study, a numerical study is performed to one plain and six circular tubes with discrete ribs in two arrangements; in-line and staggered. Air is used as a working fluid at $3{,}600 \le Re \le 16{,}525$. The number of ribs is changed from 4 to 12 to study its effect on heat transfer rate (HTR) and pressure drop (ΔP). PEC is performed to estimate the thermal hydraulic efficiency (THE) for the all test tubes. The flow phenomena and temperature contours are shown to illustrate the temperature distribution and vortices.

ملخص البحث

فى هذا البحث, تم اجراء دراسة عدديه لانبوب دائرى املس بالاضافة لعدد ستة انابيب مزوده بنتوئات مرتبه على صف واحد و صف متداخل. تم استخدام الهواء داخل الانبوب عند عدد رينولدز ما بين ٣,٦٠٠ الي ١٦,٥٢٥. تم تغيير عدد النتوئات من ٤ الي ١٢ لدراسة تاثير تغيير العدد على معدل انتقال الحراره وفقد الضغط. معامل تقييم الاداء تم استخدامه لدراسه الكفاءة الهيدروحرارية لجميع الانابيب المستخدمة فى الدراسة. تدريج درجة الحراره وشكل السريان داخل الانابيب تم عرضه بشكل واضح لتوضيح شكل الدومات المتكونة حول النتوئات بالاضافه الي توزيع الحراره داخل الانبوب.

Keywords

Ribs, Heat transfer enhancement, Vortices, CFD

Nomenclature

A	Tube inside surface area, m^2.	Re	Reynolds number.
c_p	Air specific heat at constant pressure, J/kg. K.	T	Temperature.
d	Tube inner diameter, m.	u	Average air velocity, m/s.
e	Rib depth, m.	ΔP	Pressure drop, Pa.
f	Friction factor.	ρ	Density, kg/m^3.
h	Heat transfer coefficient, W/m^2K.	μ	Air dynamic viscosity, Pa. s
L	Tube length, m.	**Subscripts**	
$\dot{m}$	Air mass flow rate, kg/s.	i	Inlet.
N	Peripheral ribs number	o	Outlet.
Nu	Nusselt number.	s	Surface.
PEC	Performance evaluation criteria.	b	Bulk.
p	Rip pitch, m.	0	Reference tube (plain tube).
Q	Heat transfer rate in the tube, W.		

1. Introduction

Heat exchangers can be found in a lot of engineering applications; such as chemical industries and refrigeration. So, the heat transfer enhancements are very important to reduce their size and cost. Active and passive techniques are a common technique that used in heat transfer enhancement. Active technique depending on the external power source while the passive one can be performed by two methods; one by making modifications in heat exchanger internal surface such as grooves, while the other is obtained by inserting different tape shapes inside the tube such as coiled-wires and conical rings.

Naphon [1] experimentally, studied the effect of inserting a twisted-tape inside double pipe heat exchanger on HTR and ΔP. Water was used as a working fluid at $7{,}000 \le Re \le 23{,}000$. Results showed that the HTR increased up to three than that for the plain tube. Eiamsa-ard et al. [2] experimentally, studied the effect of inserting full and short length twisted-tape on HTR and ΔP by using air as a working fluid at $4{,}000 \le Re \le 20{,}000$. Results showed that the full-length twisted-tape has a higher enhancement efficiency (EE) than that for the short-length one.

Muñoz-Esparza and Sanmiguel-Rojas [3] numerically; investigated the effect of inserting a helically coiled-wire inside the heat exchanger tube on HTR and ΔP. Water and water-propylene glycol was selected as a working fluid at $50 \le Re \le 850$. The HTR increases by 2.5 times than that for the plain tube.

Pethkool et al. [4] experimentally; studied the effect of using a helically-corrugated tube instead of a plain one in the heat exchanger on HTR and ΔP. The air was selected as a working fluid at $5{,}500 \le Re \le 60{,}000$. Nusselt number (Nu) and friction factor (*f*) increased up to 3.01 and 2.14 times than that for the plain tube. Bilen et al. [5] performed an experimental study by using air as a working fluid at $10{,}000 \le Re \le 38{,}000$ for circular, trapezoidal and rectangular groove shapes. Results showed that the obtained HTR is up to 63%, 58% and 47% for circular, trapezoidal and rectangular groove, respectively than that for the plain one.

Zdaniuk et al. [6] experimentally; studied eight helically-finned tubes and one plain tube using water as a working fluid at $12{,}000 \le Re \le 60{,}000$. The HTR increased by up to 2 times than that for the plain one. Zheng et al. [7-11] numerically; studied the effect of discrete ribs and grooves as inclined or straight orientation on Nu and *f* at $6{,}800 \le Re \le 20{,}340$. Several parameters for ribs/grooves were chosen to study their effect on HTR and ΔP. This study showed that ribs gave higher THE than that for grooves or ribs/grooves combinations. Also, inclined ribs or grooves have better THE than that for straight ones. The maximum THE is 2.3 for inclined ribs.

Huang et al. [12] studied, experimentally, the effect of ring-type ribs on HTR and ΔP. Air and water were selected as a working fluid at $3{,}601 \le Re \le 16{,}525$. Results obtained from Huang et al. showed that the THE increased by up to 1.5 times than that for the plain tube. Sayed Ahmed et al. [13] showed that the ring type ribs gave higher THE than that for rectangular, triangular and trapezoidal ribs. Results also showed that the ring type ribs gave highest exergy efficiency.

García et al. [14] studied the effect of coiled-wire inserts, corrugated and dimpled tube to investigate its effect on HTR and ΔP. They claimed that the plain tube gave the highest THE at $Re \le 200$. The coiled wire inserts were recommended at $200 \le Re \le 2{,}000$ while the corrugated and dimpled tubes are recommended at $Re \ge 2{,}000$. Thianpong et al. [15] revealed that both heat transfer coefficient (h) and *f* in the dimpled tube fitted with the twisted tape, were higher than those in the dimple tube acting alone and the plain tube.

2. *Model description*

The present numerical study is performed on six ribbed tubes and one plain tube. The tested tubes are 1.08 m length (L), 13.8 mm inner diameter (d) and 2 mm rib width. The rib-depth to tube-inner-diameter ratio (e/d) is 0.069 and pitch to tube inner-diameter ratio (p/d) is 1.45 while the peripheral ribs numbers (N) are 4,8,12. In-line and staggered arrangements are used to arrange the ribs along the tested tubes. Air is used as a working fluid and entering the tube at 298k with $3{,}600 \le Re \le 16{,}525$. A constant surface temperature equal to 373K is applied to the surface of the tested tubes. **Figure 1** shows the schematic drawing of the tested tubes.

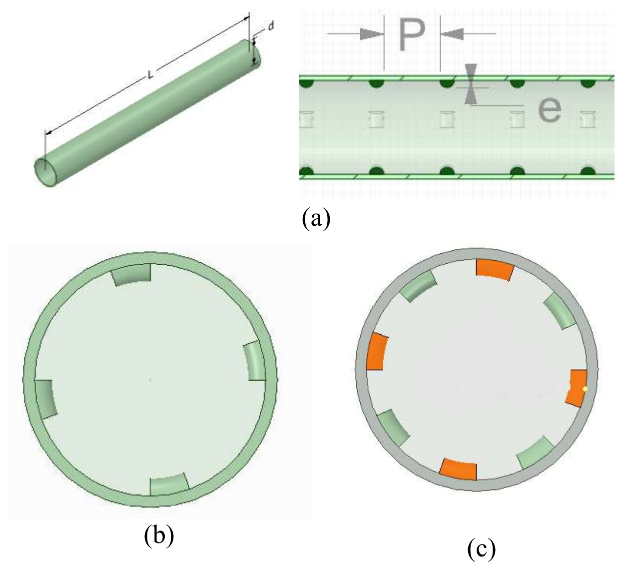

Fig. 1 schematic drawing for the test tube: (a) tube dimensions (d) In-line arrangement (c) staggered arrangement.

3. *Data reduction*

The correlations that used to obtain Re, h, Nu, *f* and PEC are listed below:

$$h = \frac{Q}{A_s (T_s - T_b)} = \frac{\dot{m} c_p (T_o - T_i)}{(\pi d L)(T_s - T_b)} \quad (1)$$

$$\mathrm{Nu} = \frac{\mathrm{h} \times \mathrm{d}}{\mathrm{k}} \tag{2}$$

$$f = \frac{2 \times \Delta \mathrm{P} \times \mathrm{d}}{\rho \times \mathrm{L} \times \mathrm{u}^2} \tag{3}$$

$$\mathrm{Re} = \frac{\rho \times u \times d}{\mu} \tag{4}$$

$$\mathrm{PEC} = \frac{(\mathrm{Nu} / \mathrm{Nu}_0)}{(f / f_0)^{1/3}} \tag{5}$$

4. *Numerical model*

The commercial CFD software ANSYS Fluent 17.0 [16] is applied to perform this numerical analysis. ANSYS design modular is used to generate a mesh for all tested tubes. A mesh independence solution is performed to ensure that the solution does not change with mesh changing. Figure 2 shows the mesh shape for in-line tested tube as a sample of mesh. Boundary layer mesh is used near the tube wall and the tape inserts to confirm that the dimension of the first cell next to the walls to get high accuracy results as recommended in [17-18].

The selection of an appropriate turbulence model is a serious part of the solution accuracy. The RNG k-ε model and Realizable k-ε model are two common turbulence models in heat transfer applications. These two models are considered to investigate the numerical solution for Nu and *f*. Experimental results, obtained from [12], are employed to make a comparison with numerical ones obtained from these turbulent models. Figure 3 illustrates the numerical and experimental validation results for Nu and *f*. It also shows that the RNG k-ε model gave an approximate result to experimental ones.

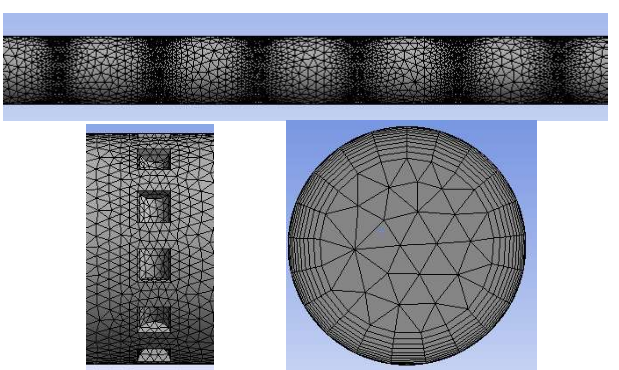

Fig. 2 Mesh shape for the test tubes.

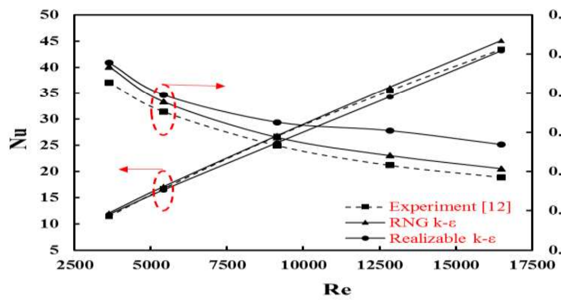

Fig. 3 Experimental and numerical validation results for Nu and *f*.

The flow field is governed by the 3D Reynolds averaged Navier-Stokes (RANS) equations. There are some assumptions are suggested to simplify these equations. These assumptions are that the heat transfer and fluid flow processes are steady-state and turbulent. Also, the heat loss to the environment is neglected. The governing equations are:

- **Continuity**

$$\frac{\partial}{\partial x_i}(\rho U_i) = 0.0 \tag{6}$$

- **Momentum**

$$\frac{\partial\left(\rho \overline{u_i u_j}\right)}{\partial x_j} = -\frac{\partial p}{\partial x_i} + \frac{\partial}{\partial x_j}\left(\mu\left(\frac{\partial u_i}{\partial x_j} + \frac{\partial u_j}{\partial x_i}\right)\right) - \frac{\partial(\rho}{\partial}$$

- **Energy equation**

$$\frac{\partial}{\partial x_j}\left(u_j(\rho e + p)\right) = \frac{\partial}{\partial x_j}\left(k\frac{\partial T}{\partial x_j}\right) \tag{8}$$

where i is a tensor indication 1 and 2 and k is the fluid effective thermal conductivity.

The k-***ε*** (RNG) turbulence model, where turbulent viscosity μ_t is predicted with enhanced wall functions for the near wall treatment, is employed as following:

$$\frac{\partial}{\partial x_i}(\rho k u_i) = \frac{\partial}{\partial x_j}\left(\left(\mu + \frac{\mu_t}{\sigma_k}\right)\frac{\partial k}{\partial x_j}\right) + P_k - \rho\varepsilon \tag{9}$$

$$\frac{\partial}{\partial x_i}(\rho \varepsilon u_i) = \frac{\partial}{\partial x_j}\left(\left(\mu + \frac{\mu_t}{\sigma_\varepsilon}\right)\frac{\partial \varepsilon}{\partial x_j}\right) + C_{1\varepsilon}\frac{\varepsilon}{k}P_k \overset{(1}{_{0)}} C_{2\varepsilon}\rho\frac{\varepsilon^2}{k}$$

where k and ε represent as the fluid turbulent kinetic energy and the dissipation rate of turbulent kinetic energy, respectively

The boundary conditions applied to the all tested tubes are shown in Fig. 4. Uniform velocity was applied to the tube inlet based on $3601 \leq Re \leq 16523$ and pressure outlet is applied to the tube outlet. A constant temperature is applied to the surface of the tested tubes. The minimum convergence criterion is set to 10^{-5} for the continuity, momentum and turbulence equations. However, it is set to 10^{-8} for the energy equation for more accurate temperature calculations.

Fig. 4 Boundary conditions applied for the all tested tubes.

5. Results and Discussion

Numerical data obtained from simulation is validated with experimental ones obtained from [12]. Figure 5 shows the experimental and numerical validation data for Nu and *f*. This figure shows that numerical results are agreed with the experimental ones, within ±3% and ±6% for Nu and *f*, respectively. As shown in this figure, with increasing in Re the Nu increases but *f* decreases.

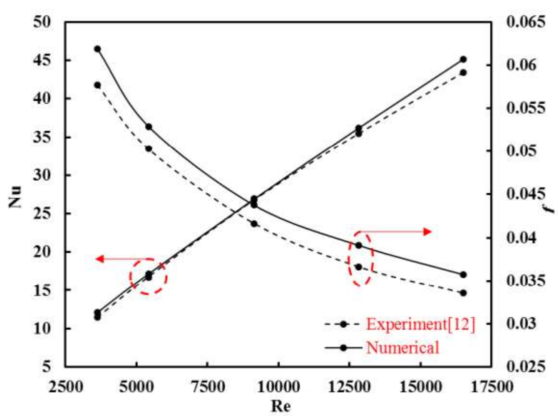

Fig. 5 Validation between experimental [12] and numerical data for plain tube.

The first numerical study is performed in an in-line arrangement for the ribs. Figure 6 shows the variation of Nu and *f* against Re. As shown in this figure Nu increases but the *f* decreases with Re increasing. The highest Nu and *f* are occurring for the tube with N=12 that mean the higher HTR and ΔP. So, the PEC is obtained for the tested tubes to assign the tube with higher THE. Figure 7 shows the variation of PEC with Re. The tube with N=4 has a higher THE. The PEC value decreases with increase in Re.

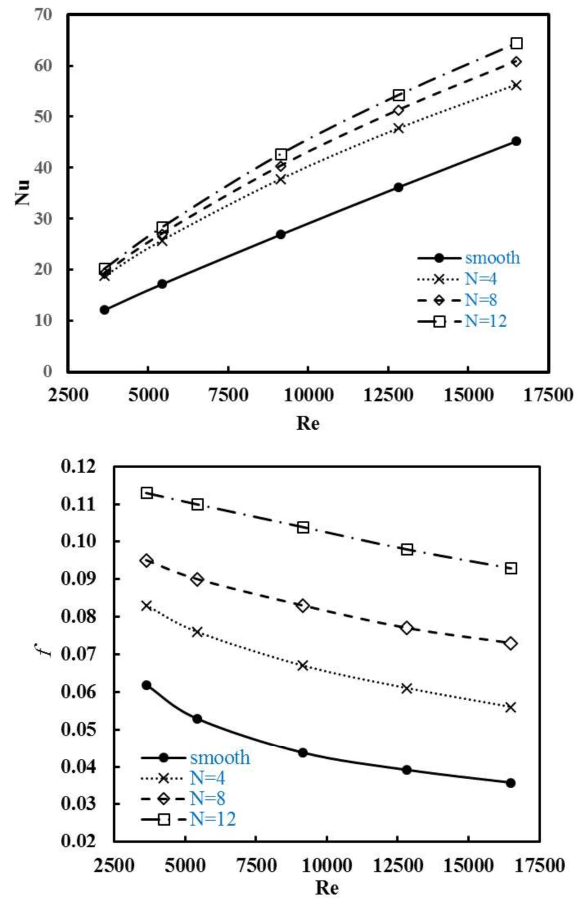

Fig. 6 Validation of Nu and *f* against Re for the in-line arrangement.

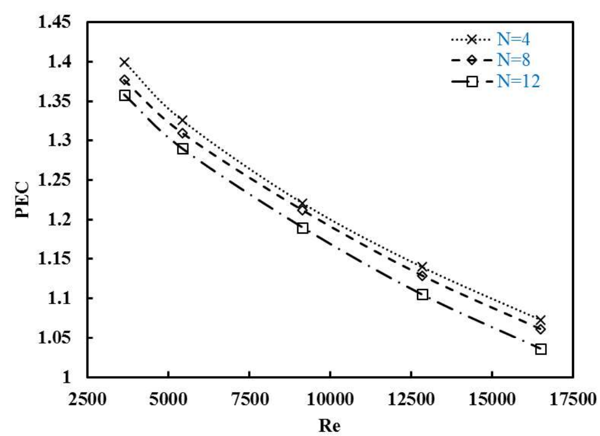

Fig. 7 The PEC values at different Re for the in-line arrangement.

The second numerical study is performed in a staggered arrangement for the ribs. Figure 8 shows the variation of Nu and *f* vs Re. As shown in this figure Nu increases but *f* decreases with Re increasing. The highest values of Nu and *f* are occurring for the tube with N=12 that mean the higher HTR and ΔP. So, PEC is obtained for the tested tubes to determine the tube with higher thermal hydraulic efficiency. Figure 9 shows the variation of PEC with Re. The tube with N=4 has a higher thermal hydraulic efficiency and the PEC value decrease with increase in Re.

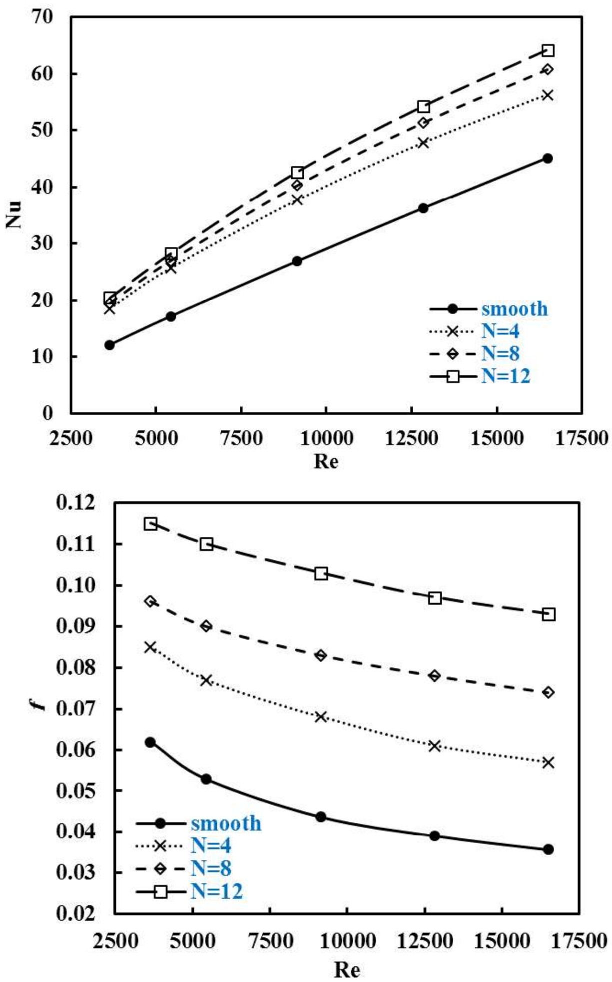

Fig. 8 Nu and *f* at different Re for staggered arrangement

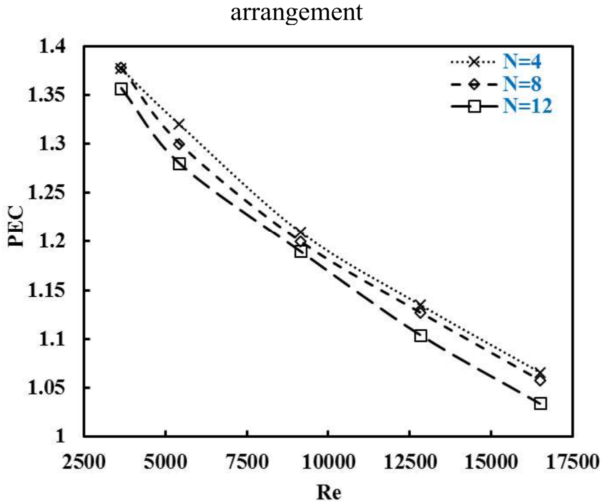

Fig. 9 The PEC values at different Re for staggered arrangement.

After performing the numerical study for two discrete ribs arrangements and obtaining the THE. It is important to determine which arrangement gives the highest THE. Figure 10 shows which arrangement gives the highest THE. As shown from this figure the staggered arrangement gives slightly higher PEC than that for the in-line one.

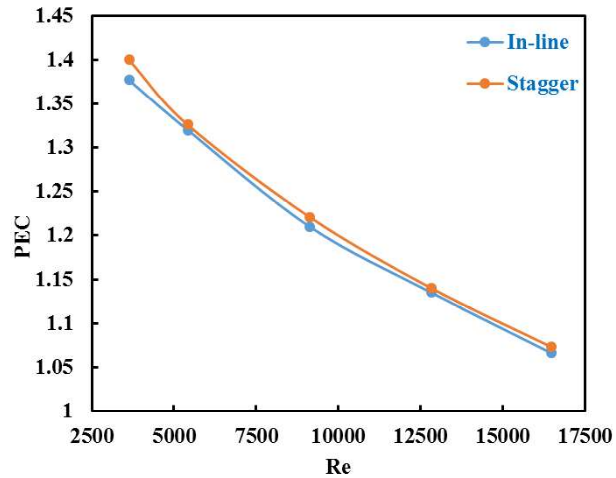

Fig. 10 Comparison between in-line and staggered arrangements at N=4.

Temperature and velocity contours with flow streamlines are represented for the tested tubes. All temperature and velocity contours as well as streamlines represented at Re=12,833. Figures 11 and 12 show the temperature contours for in-line and staggered arrangements at N=4, respectively. It is clear from these figures that the temperature increases from the tube surface to the tube core. Ribs cause flow disturbance that enhances the mixing between the cold and hot fluid. There is no huge difference between in-line and staggered arrangements in temperature contours.

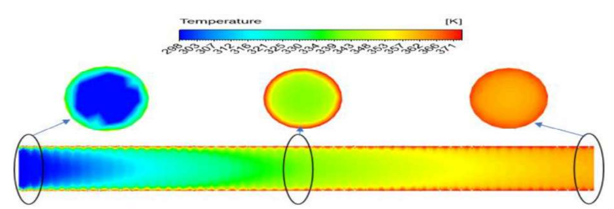

Fig. 11 Temperature contours for the tube with the in-line arrangement at inlet, outlet and mid-sections.

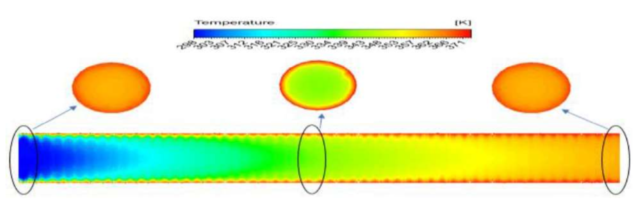

Fig. 12 Temperature contours for the tube with the staggered arrangement at inlet, outlet and mid-sections.

Figure 13 shows the velocity contours at two arrangements. As shown in this figure there are a lot of vortices. These vortices cause disturbance to the flow and discontinuity in the hydraulic boundary layer. This leads to the enhancements in HTR but increase ΔP.

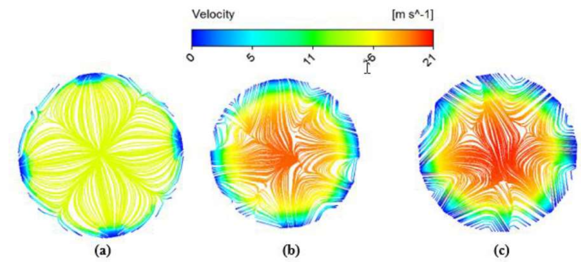

In-Line arrangement

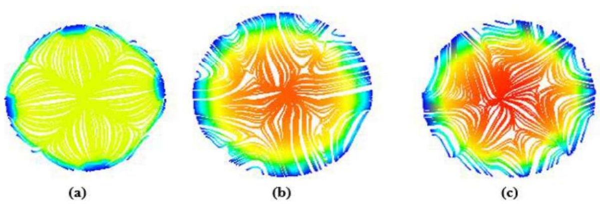

Stagger arrangement

Fig. 13 Velocity contours for the two arrangements.

6. Conclusions

In the present work, a numerical study is performed on a plain tube, three in-line discrete ribbed tubes and three stagger discrete ribbed tubes using the RNG k-ε turbulence model with enhanced wall treatments. The Nu, f and PEC characteristics of all tested tubes are investigated. Temperature and velocity contours are presented.

Results of this work are summarized as: -

- Nu and f increase with increasing in ribs number.
- The increasing in Re led to increase in Nu but decrease in f.
- The tubes with N=4 in staggered or in-line arrangements have a higher PEC.
- The heat transfer increases up to 150-200% and friction factor increase up to 190-250%.
- Max PEC is 1.4 for stagger arrangement.
- Stagger arrangement better than in-line arrangements.

References:

[1] Paisarn Naphon. Heat transfer and pressure drop in the horizontal double pipes with and without twisted tape insert. International Communications in Heat and Mass Transfer 33 (2006) 166–175.

[2] Smith Eiamsa-ard, Chinaruk Thianpong, Petpices Eiamsa-ard, Pongjet Promvonge. Convective heat transfer in a circular tube with short-length twisted tape insert. International Communications in Heat and Mass Transfer 36 (2009) 365–371.

[3] D. Muñoz-Esparza, E. Sanmiguel-Rojas. Numerical simulations of the laminar flow in pipes with wire coil inserts. Computers & Fluids 44 (2011) 169–177.

[4] . Pethkool, S. Eiamsa-ard, S. Kwankaomeng, P. Promvonge, Turbulent heat transfer enhancement in a heat exchanger using helically corrugated tube, International Communication of Heat Mass Transfer 38 (2011) 340–347.

[5] Kadir Bilen, Murat Cetin, Hasan Gul, Tuba Balta. The investigation of groove geometry effect on heat transfer for internally grooved tubes. Applied Thermal Engineering 29 (2009) 753–761.

[6] Gregory J. Zdaniuk, Louay M. Chamra, Pedro J. Mago. Experimental determination of heat transfer and friction in helically-finned tubes. Experimental Thermal and Fluid Science 32 (2008) 761–775.

[7] N. Zheng, W. Liu, Z. Liu, P. Liu, F. Shan, A numerical study on heat transfer enhancement and the flow structure in a heat exchanger tube with discrete double inclined ribs, Applied Thermal Engineering 90 (2015) 232-241.

[8] N. Zheng, P. Liu, F. Shan, Z. Liu, W. Liu, Effects of rib arrangements on the flow pattern and heat transfer in an internally ribbed heat exchanger tube, Int. J. of Thermal Sciences 101 (2016) 93-105.

[9] N. Zheng, P. Liu, F. Shan, Z. Liu, W. Liu, Turbulent flow and heat transfer enhancement in a heat exchanger tube fitted with novel discrete inclined grooves, Int. J. of Thermal Sciences 111 (2017) 289-300.

[10] N. Zheng, P. Liu, F. Shan, Z. Liu, W. Liu, Numerical investigations of the thermal-hydraulic performance in a rib-grooved heat exchanger tube based on entropy generation analysis, Applied Thermal Engineering 99 (2016) 1071–1085.

[11] N. Zheng, P. Liu, F. Shan, Z. Liu, W. Liu, Heat transfer enhancement in a novel internally grooved tube by generating longitudinal swirl flows with multi-vortexes, Applied Thermal Engineering 95 (2016) 421–432.

[12] Wen-Chieh Huang, Cheng-An Chen, Chi Shen, Jung-Yang San. Effects of characteristic parameters on heat transfer enhancement of repeated ring-type ribs in circular tubes. Experimental Thermal and Fluid Science 68 (2015) 371–380.

[13] Sayed Ahmed E. Sayed Ahmed, Emad Z. Ibrahim, Mostafa M. Ibrahim, Mohamed A. Essa, Mohamed A. Abdelatief, Mohamed N. El-Sayed, Heat transfer performance evaluation in circular tubes via internal repeated ribs with entropy and exergy analysis, Applied Thermal Engineering 144 (2018) 1056–1070.

[14] A. García, J.P. Solano, P.G. Vicente, A. Viedma. The influence of artificial roughness shape on heat transfer enhancement: Corrugated tubes, dimpled tubes and wire coils. Applied Thermal Engineering 35 (2012) 196-201.

[15] Chinaruk Thianpong, Petpices Eiamsa-ard, Khwanchit Wongcharee, Smith Eiamsa-ard. Compound heat transfer enhancement of a dimpled tube with a twisted tape swirl generator. International Communications in Heat and Mass Transfer 36 (2009) 698–704.
[16] ANSYS 17.0 CFD software ©;2015
[17] Mansour, N., J. Kim, and P. Moin, Near-wall k-epsilon turbulence modeling. AIAA journal, 1989. 27(8): p. 1068-1073.
[18] Mohammadi, B. and O. Pironneau, Analysis of the k-epsilon turbulence model. 1993: Editions MASSON; Paris (France).